Available online at www.sciencedirect.com
SCIENCE DIRECT
Journal of Solid State Chemistry 179 (2006) 1698–1706
JOURNAL OF SOLID STATE CHEMISTRY
www.elsevier.com/locate/jssc

Microstructural and transport properties in substituted $Bi_2Sr_2CaCu_2O_{8+\delta}$-modulated compounds

C. Autret-Lambert[a,*], B. Pignon[a], M. Gervais[a], I. Monot-Laffez[a], A. Ruyter[a], L. Ammor[a], F. Gervais[a], J.M. Bassat[b], R. Decourt[b]

[a]*LEMA UMR 6157 CNRS-CEA, Faculté des Sciences et Techniques, Université François Rabelais, Parc Grandmont, 37200 Tours, France*
[b]*ICMCB CNRS UPR 9048, Université de Bordeaux I, 87 av. du Dr Schweitzer, 33608 Pessac cedex, France*

Received 3 January 2006; received in revised form 3 March 2006; accepted 5 March 2006
Available online 12 March 2006

Abstract

X-ray powder diffraction and resistivity measurements were performed on $Bi_2Sr_2CaCu_2O_{8+\delta}$ ceramics substituted by Y and Zn for Ca and Cu sites, respectively. X-ray diffraction patterns show an incommensurate modulated structure along the *b*-axis. The structural refinements were carried out using the four-dimensional space group $Bbmb(0\beta1)0\,0\,0$. From the X-ray peak profiles analysis, an anisotropic line-shape broadening was observed. The use of the ''Williamson and Hall'' method allows distinguishing the origin of broadening as mainly due to microstrains. A large transition from a metallic to semiconductor behaviour is observed on the resistivity curves at $x \approx 0.4$ for $Bi_2Sr_2Ca_{1-x}Y_xCu_2O_{8+\delta}$ and at $x' \approx 0.36$ for $Bi_2Sr_2Ca_{1-x}Y_xCu_{1.94}Zn_{0.06}O_{8+\delta}$, which can be also correlated to the defects. Oppositely to the metallic behaviour, which satisfies the Mathiessen's rule, the semiconducting one can be modelled by a variable range hopping process.

Keywords: Bi-based cuprates; X-ray diffraction; Experimental determination of defects by diffraction; Transport properties

1. Introduction

Many experiments have been performed in order to understand the superconductivity mechanism observed in cuprate high-temperature superconductors [1]. All these cuprates generally contain pseudo-square network of $[CuO_2]$ layers and the superconducting transition temperature T_C shows highest value for large stacks of superconducting planes (at least up to 3). The superconductivity also depends on hole concentration, i.e. the Cu^{3+}/Cu^{2+} ratio in these compounds. Among all materials, the $Bi_2Sr_2CaCu_2O_{8+\delta}$ compound (denoted Bi2212) is an interesting candidate to obtain high-temperature superconductivity with T_C close to 90 K. The diffraction pattern associated to this compound exhibits two types of reflections, main reflections showing usually stronger intensities and extra reflections with weak intensities. In order to obtain an accurate description of the structure, the whole reflections should be indexed considering the modulation vector $\mathbf{q}^* = \beta\mathbf{b}^* + \mathbf{c}^*$ with $\beta \sim 0.21$. The structure generally resolves from single crystal analysis using four-dimensional (4D) superspace formalism [2] and could be described like a modulated structure [3–7] or like a composite one, i.e. like two alternated sublattices along the [001] direction [8,9]. All studies have shown that the structure corresponds to the alternation of ''NaCl''-type layers ([BiO]) and pseudo-perovskite-type layers ([SrO], [CaO] and [CuO]) along the stacking axis. The lattice mismatch of these planes is responsible for both appearance of an incommensurate modulation and disorder phenomena [3].

The 2D electronical and physical behaviours observed for the Bi2212-type compounds could be related to the pseudo-2D framework of this material. Several authors have attempted to determine the extra oxygen inserted in the [BiO] layers. It is now well established that the variation of oxygen content and the distribution of oxygen atoms in

*Corresponding author. Fax: +33 2 47 36 71 21.
E-mail address: cecile.autret@univ-tours.fr (C. Autret-Lambert).

0022-4596/$ - see front matter © 2006 Elsevier Inc. All rights reserved.
doi:10.1016/j.jssc.2006.03.005

the lattice sites strongly influence the physical and structural properties of high-temperature superconductors and many other oxides [10]. It is believed that this compound has a much smaller range of oxygen non-stoichiometry than the $YBa_2Cu_3O_{7-\delta}$ system [11] and that this non-stoichiometry probably induces many defects in these samples.

Recently, it has been pointed out from inelastic neutron scattering experiments that dynamical stripe correlations of spins and holes exist in a wide range of hole concentration in La_2CuO_4 [12] and also in Bi2212 [13] phases. However, when the dynamical stripes are pinned by special crystal structures (e.g. the tetragonal low-temperature structure in La_2CuO_4 or a small amount of Zn or Ni in Bi2212) to become a quasi-static stripe order at $p \approx \frac{1}{8}$ (p: hole concentration per Cu in the CuO_2 plane), the superconductivity is suppressed [14]. Therefore, the so-called "1/8 anomaly" is expected to appear in Bi2212 and $YBa_2Cu_3O_{7-\delta}$ phases when adequate pinning centres are introduced into a sample.

On the one hand, to vary the carrier's concentration, we have doped Bi2212 with yttrium (Y^{3+}) on calcium site, i.e. in the "perovskites" planes: $Bi_2Sr_2Ca_{1-x}Y_xCu_2O_{8+\delta}$. On the other hand, Akoshima et al. [15] have studied the effects of Cu substitution by Zn, that is a superconductivity killer. They have observed, as expected, an anomalous depression of the superconducting transition for the $Bi_2Sr_2Ca_{1-x'}Y_{x'}Cu_{2-y}Zn_yO_{8+\delta}$ with $x' \approx 0.3-0.35$ and $y = 0.05-0.06$. According to these authors, Zn will act as pinning centres for dynamical stripes. This suggestion has been proposed in comparison with Tranquada's work [14] which showed that stripes become static when pinned by structural effects linked to the neodymium content in $La_{2-x-y}Nd_ySr_xCuO_4$. This is why the effect of Zn substitution in Bi2212 deserves careful investigation.

In this work, we studied the influence of substitutions like Ca/Y and Cu/Zn on the structural, microstructural and physical properties of Bi2212 compound. The $Bi_2Sr_2Ca_{1-x}Y_xCu_2O_{8+\delta}$ and $Bi_2Sr_2Ca_{1-x'}Y_{x'}Cu_{1.94}Zn_{0.06}O_{8+\delta}$ are denoted Y_x and $ZnY_{x'}$, respectively.

2. Experimental

$Bi_2Sr_2Ca_{1-x}Y_xCu_2O_{8+\delta}$ (Y_x) and $Bi_2Sr_2Ca_{1-x'}Y_{x'}Cu_{1.94}Zn_{0.06}O_{8+\delta}$ ($ZnY_{x'}$) samples were prepared by an organic gel-assisted citrate process [16,17]. The obtained gel was calcined in air at 750 °C for 5 h to give an intermediate black powder. This treatment allows the degradation of organic compounds. Then, the formation of the Bi2212 phase consists in two sinterings in air at 860 °C for 12 h with intermediate grindings in an agate mortar.

Compositions were checked by energy dispersive X-ray (EDX) and wavelength dispersive X-ray (WDX). Thermogravimetric measurements were carried out in Ar/H_2 (10%) atmosphere and alumina crucibles with heating/cooling of 5 °C/min at 600 °C. The oxygen rate was difficult to determine because of the appearance of Bi_2O_3. However, this investigation exhibits that the rate is constant with Y substitution.

X-ray diffraction (XRD) was carried out using a Bruker D8 X-ray diffractometer using Cu$K\alpha$ radiation. The diffraction pattern analysis was operated using the Jana2000 program [18]. Resistivities were measured with a standard dc four-point probe method, and T_C is defined from the resistivity curves as the onset of the transition.

3. Results

All powder samples were examined with the use of powder XRD technique. The different X-ray patterns

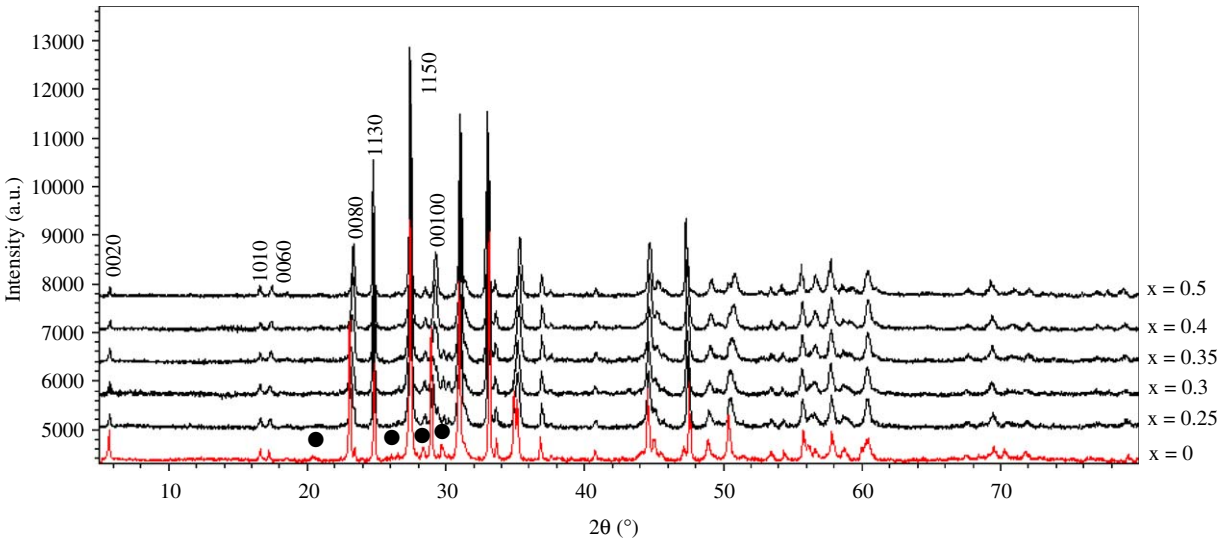

Fig. 1. Powder X-ray diffraction patterns of $Bi_2Sr_2Ca_{1-x}Y_xCu_2O_{8+\delta}$ compounds (noted Y_x in the text). The main reflections are indexed $hklm$ ($m = 0$) and the satellite reflections denoted by ●.

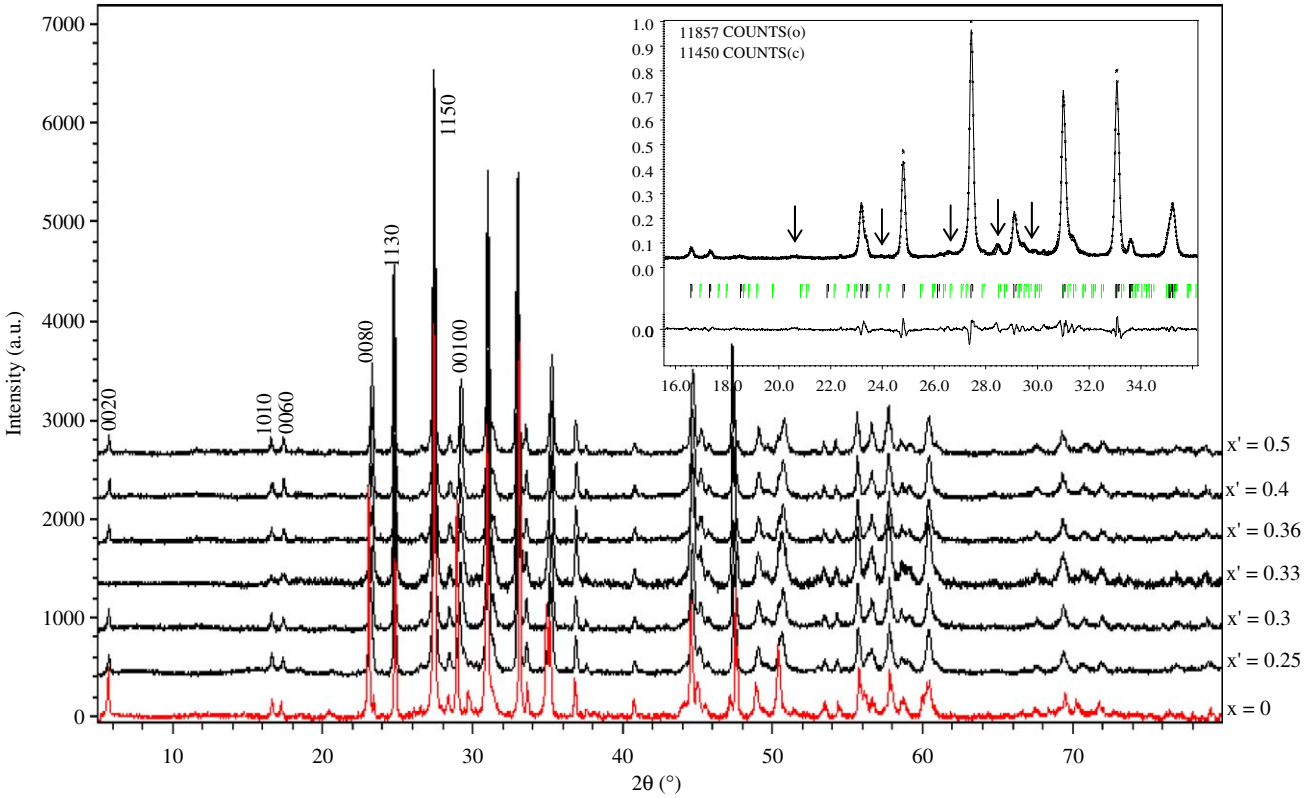

Fig. 2. Powder X-ray diffraction patterns of $Bi_2Sr_2Ca_{1-x'}Y_{x'}Cu_{1.94}Zn_{0.06}O_{8+\delta}$ compounds (noted $ZnY_{x'}$ in the text). In inset enlarged refinement of $Bi_2Sr_2Ca_{0.75}Y_{0.25}Cu_{1.94}Zn_{0.06}O_{8+\delta}$ with the modulation peaks denoted by arrows.

measured for the Y_x and $ZnY_{x'}$ compound families are shown in Figs. 1 and 2, respectively. It can be seen that diffraction patterns possess the undoped Bi2212-type layered structure and do not exhibit any extra reflections due to an impurity phase. In order to obtain an accurate description of the doping agent effects, the diffraction patterns were refined using the superspace formalism [2]. All observed reflections can be indexed considering the diffraction vector $\mathbf{s}^* = h\mathbf{a}^* + k\mathbf{b}^* + l\mathbf{c}^* + m\mathbf{q}^*$, where m is the satellite order. The conditions observed for the whole reflections are consistent with the superspace group $Bbmb(0\beta1)000$, β close to 0.21, usually observed for the study of Bi2212-type compounds [3–7]. The Bi2212 undoped compound diffraction pattern was compared with the simulated pattern using the Yamamoto model [6]. The intensities ratio has been checked and exhibited that the structural framework is compatible with this model. The reliability factors are close to $R_p = 4.32\%$, $R_{wp} = 6.51\%$ and gof (goodness of fit) $= 1.56$. No modulated structure refinement was performed due to the weak intensity and large broadening of the satellite diffraction peaks.

However, structural parameters could be obtained and permit to determine the influence of doping agent on the structural network. Figs. 3 and 4 show the variation of lattice parameters a, b, c and the volume of the unit cell for the Y_x and $ZnY_{x'}$ series. In all cases the reliability factors are for R_p and R_{wp} lower than 10% and for gof lower than 2.5 and the refined cell parameters ($a \approx 5.40$ Å, $b \approx 5.41$ Å and $c \approx 30.70$ Å) are consistent with the literature [3–7,19]. Substituting only Y for Ca preserves the basic crystalline structure, with an orthorhombic symmetry, while decreasing the c-axis parameter and increasing slightly both in plane parameters. The c value evolution, already observed in the literature [20,21], is expected from simple ionics considerations. Indeed, Y^{3+} cation has a smaller size compared to the Ca^{2+} ion, 1.075 and 1.180 Å, respectively. However, the slight increase of a and b is more complex, since the a-axis length is controlled by the in-plane Cu–O bond distance. This increase of the a parameter may be controlled by the hole concentration [22,23]. Indeed, as the carrier concentration decreases, the number of Cu^{3+} ions, which form a shorter Cu–O bond length compared to Cu^{2+}, decreases. In the Y_x-type compounds, the oxygen content (noted $8+\delta$) changes with the concentration of the substituting cations (Y^{3+}). Consequently, the average valence of Cu (denoted $2+p$) also changes. Previous experimental results exhibit the decrease of the average valence of Cu with Y content, explaining the trend of a and b parameters [24]. Concerning the $ZnY_{x'}$ series, the variation of lattice parameters is similar to the previous series, i.e. without Zn. The compounds always display an orthorhombic distortion, the volume dependence tends to decrease as a function of x but an anomaly is observed for

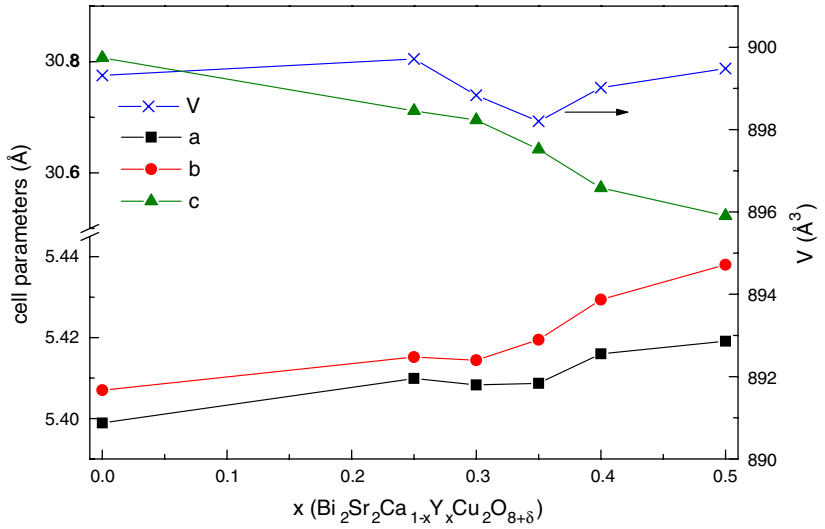

Fig. 3. Cell parameters (left axis) and volume (right axis) at room temperature as a function of x in Y_x. Note that the error bars are smaller than the size of the symbols.

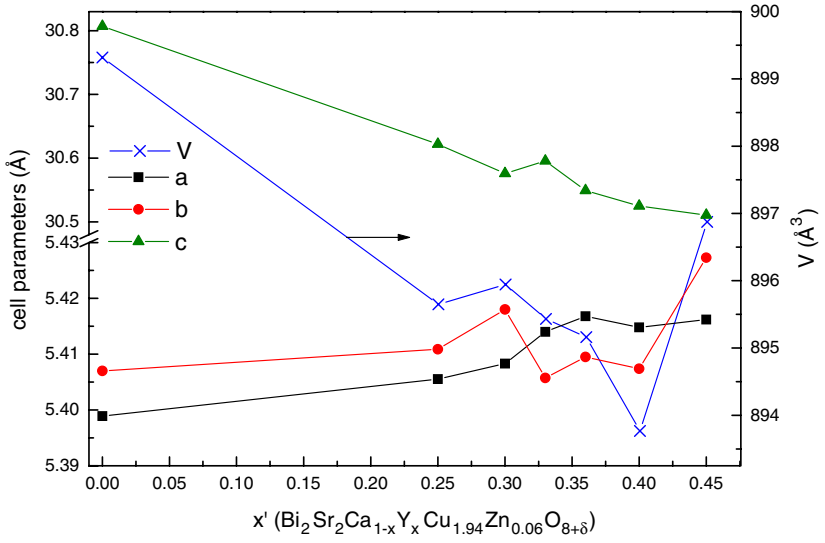

Fig. 4. Cell parameters (left axis) and volume (right axis) at room temperature as a function of x' in $ZnY_{x'}$. Note that the error bars are smaller than the size of the symbols.

$0.3 < x < 0.4$ with an inversion of a and b. These compositions correspond to the anomalous depression observed by Akoshima [15].

It has been shown that the bulk of high-T_C superconductors contains a lot of defects [25 and references herein]. Most of these defects are due to intergrowths along the c-stacking direction, to the cationic disorder but also to the local oxygen non-stoichiometry inducing distortions in the structure at the atomic scale [6]. Moreover, the modulation vector depends on the extra oxygen ratio in the [BiO] layers [26]. Nevertheless, some information concerning the microstructure of the compounds could be obtained from the XRD diagrams. The instrumental resolution was determined using a NIST Si powder (Fig. 5). For all diffraction patterns, the peak profile was fitted with the pseudo-Voigt profile. All measured FWHM (full-width at half-maximum) values are larger than the instrumental resolution (Fig. 5). In order to estimate the origin of this broadening, we plot $\beta \cos\theta/\lambda$ versus $\sin\theta/\lambda$, with β the FWHM sample corrected of the FWHM instrumental and λ the wavelength of X-ray Cu radiation as proposed by Williamson and Hall, an example for Y_{50} is presented in inset in Fig. 5. This method allows relating the measured peak widths to the mean crystallite size and the distribution in d spacing [27]. The results exhibit a crystallite size larger than 200 nm depending on the composition. It could be considered that the broadening comes mainly from microstrains due to the probable presence of structural defects inside the structure framework. For Y_x, the substitution leads to an increase in defects ratio with regard to the undoped compound (Fig. 5). This FWHM evolution shows that the compounds

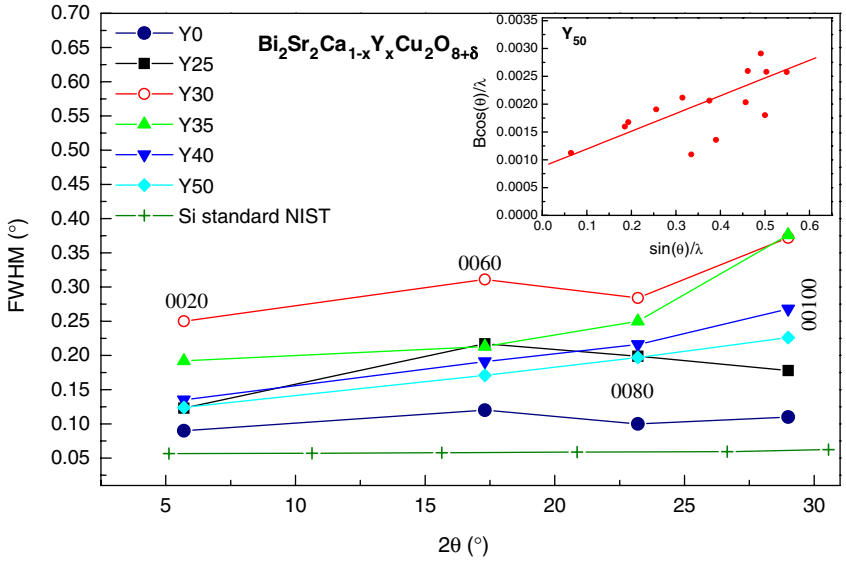

Fig. 5. 2θ dependence of half width (FWHM) for the 0 0 1 type of reflections for the NIST Si powder, undoped and Y_x compounds. Inset, the Williamson and Hall plot for $Bi_2Sr_2Ca_{05}Y_{0.5}Cu_2O_{8+\delta}$.

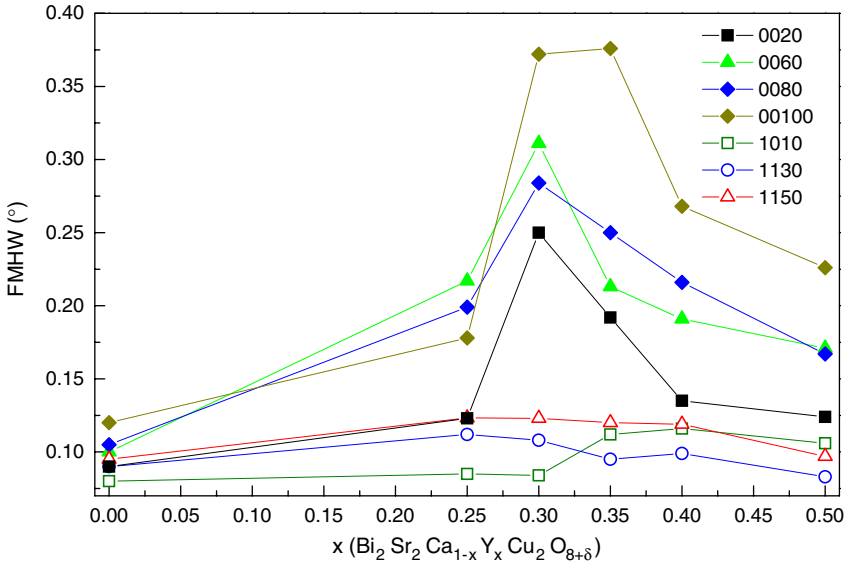

Fig. 6. FWHM as a function of x in Y_x series for different (hkl) reflections.

$Y_{0.3}$ and $Y_{0.35}$ contain more defects than the others. For the $ZnY_{x'}$ samples, the diffraction peak profile shows about the same width except the compound containing $ZnY_{0.33}$, which exhibits a high FWHM. It should be noted that the (200) peak associated to this compound is not detected in the diffraction pattern probably due to its broadening and its very weak intensity. Unfortunately, the nature of defects in these materials (Y_x and $ZnY_{x'}$) cannot be resolved by XRD analysis but some information concerning the anisotropy of their distribution could be obtained. Indeed, Figs. 6 and 7 exhibit the FWHM measured for the different (hkl) planes versus the x and x' substituting ratio in the Y_x and $Zn_{0.06}Y_{x'}$ series. It should be noted that the larger broadening is observed for the (001) peak profiles, i.e. more defects are concentrated along the c-stacking axis. Lastly, no evolution of the **q** modulation vector is evidenced in this work. Indeed, the different defects lead to local variations of the structure, then a distribution of the **q** values around $\beta \approx 0.21$. From this remark, it is not possible to propose an accurate description of the structure for each substituted compounds. So, to distinguish between a homogeneous distribution of dopant atoms in the matrix and the presence of clusters (i.e. the type of conductivity), magnetotransport measurements have been done.

Figs. 8 and 9 show plots of resistance versus temperature for various x compositions of the Y_x and $ZnY_{x'}$, respectively. Although all the samples exhibit the ideal Bi2212 single phase and are superconductors, the charge

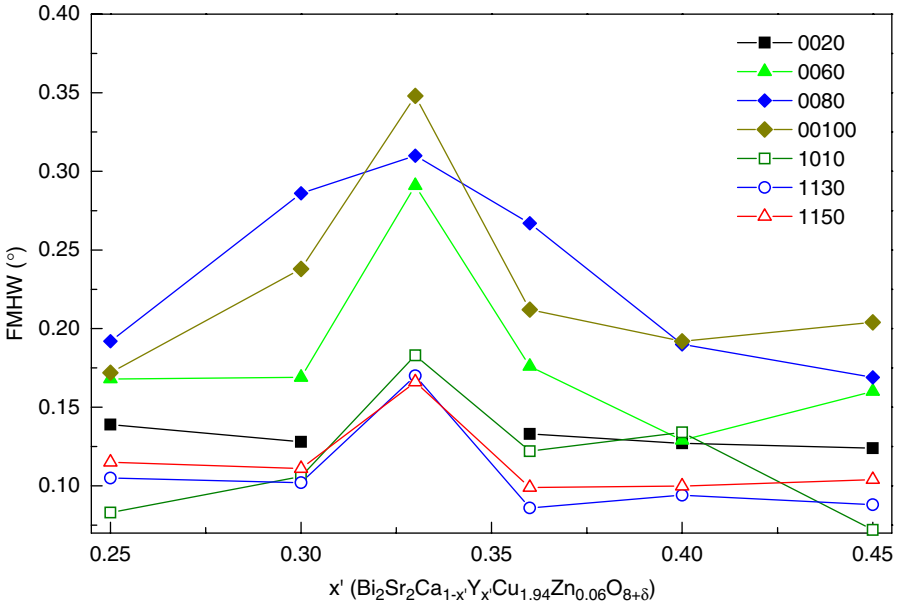

Fig. 7. FWHM as a function of x' in $ZnY_{x'}$ series for different (hkl) reflections.

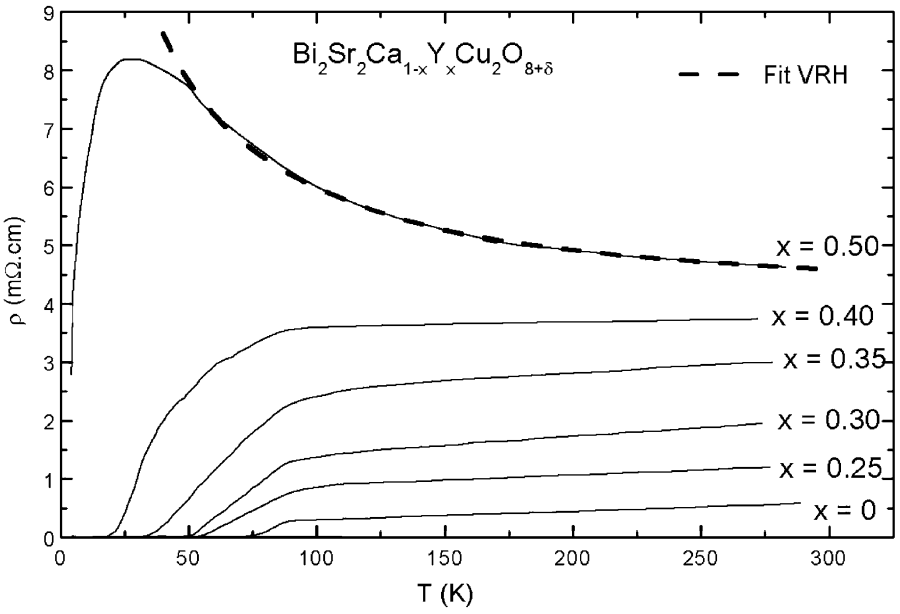

Fig. 8. Temperature dependence of the resistivity of Y_x samples.

transport properties and superconductivity are noticeably different. Above $x \approx 0.4$, the normal state changes from a metallic one ($d\rho/dT > 0$) for $T > T_C$ to a semiconducting one, with a superconducting behaviour at low temperature (Fig. 8). Finally, the $x = 0.5$ sample becomes semiconducting ($d\rho/dT < 0$) for $T > T_C$. At room temperature, the value of ρ increases with increasing x in agreement with the decreasing of hole concentration through the substitution of Y^{3+} for Ca^{2+} and leads the system into underdoped region: the superconductivity disappears around $x = 0.5$. In Fig. 9, for $ZnY_{x'}$ samples up to x' close to 0.36, the system is superconducting below T_C temperature, and the general trend of the curves sign for semiconducting-like and metallic-like regions. Then, above $x > 0.36$, the samples become semiconductor like. The (Y, Zn) substitution enhances the suppression of superconductivity faster than Y alone.

It can be noted that the superconducting transition width (ΔT_C) increases with Y doping (Figs. 8 and 9). Indeed, for the undoped compound, the transition width ΔT_C is close to 10 K whereas for $x = 0.25$ in the Y system the width is close to 30 and 50 K for $x = 0.40$. This is an indication of

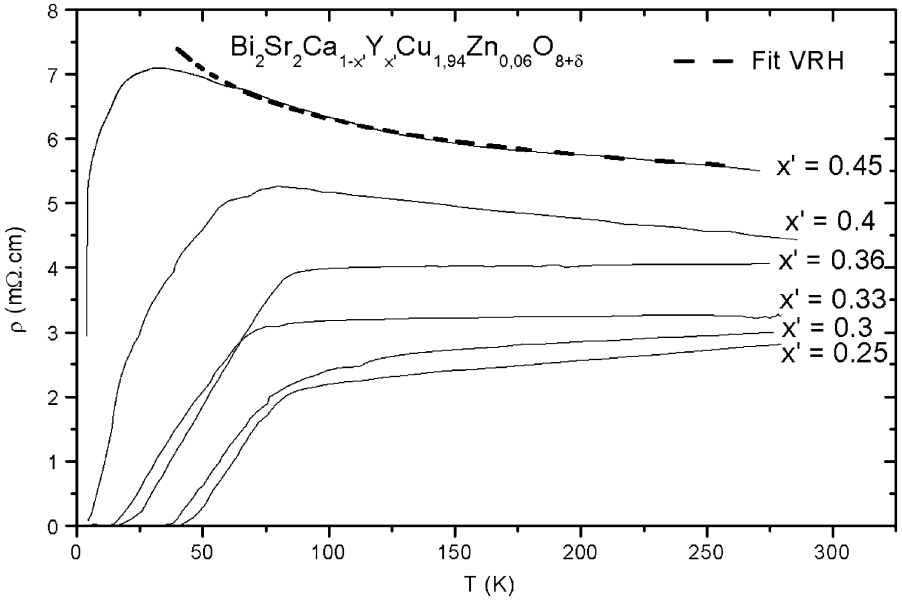

Fig. 9. Temperature dependence of the resistivity of $ZnY_{x'}$ compounds.

the homogeneity of the powders, which decreases as the dopant content increases. For metallic samples, the interpretation of the resistivity data was derived from the Matthiessen's rule which is usually used for the metals in the case of scattering by impurities. Up to x and x' close to 0.4 and 0.36, respectively, the linear part of data can then be fitted with the empirical formula:

$$\rho = \rho_0 + \alpha T, \tag{1}$$

where the residual resistivity data is $\rho_0 = m^*/ne^2\tau_0$ (m^*: effective mass of electrons and $1/\tau_0$ scattering diffusion temperature independent), and α is a constant depending on intrinsic interactions. The interpretation of ρ_0 allows to follow the scattering due to impurities [28]. The inset in Fig. 10 shows that above $x > 0.3$, the residual resistivity increases abruptly. This result can be interpreted by more defects and consequently by an increase of $1/\tau_0$. The presence of these defects, which can be also related to the large superconducting transition, is also observed by X-ray analysis in studying the FWHM evolution with doping. Some impurity scattering has been probably induced by the introduction of Y^{3+} ions into the lattice, leading to the decrease of T_C. In addition, above $x > 0.4$ and $x' > 0.36$, resistivity curves exhibit a semiconductor behaviour. These curves can be fitted with a variable range hopping (VRH) model for $T > T_C$ (Figs. 8 and 9). This model considers that some electronic states at the Fermi level are localized, and the traps are randomly distributed in energy. Thus, the conduction takes place by direct hopping of carriers from one trapping site to another with help of thermal variation of the lattice. This law is defined by the following expression:

$$\rho = c \exp(d/T)^{1/3}, \tag{2}$$

where c is a constant, d is related to both density state ($g(E_F)$) and the localization length $\frac{1}{3}$ corresponding to the dimensionality of the conduction mechanism. According to Quitmann et al. [28], this VRH behaviour is related to random distribution of Y in the Ca site. So, it can be envisaged that clusters with more Y is formed in these compounds, Y atoms could join leading to the presence of clusters.

In both systems, when the Y content increases, a loss of the superconductivity behaviour is observed (Fig. 10). The substitution of Ca^{2+} by Y^{3+} in Bi2212 introduces a reduction of the hole carrier concentration and T_C onset increases with x, except a maximum at $x \approx 0.2-0.3$, and then decreases and becomes zero beyond a critical concentration, while maintaining its single phase character [27]. In earlier studies, the decrease or disappearance of T_C was attributed to the excess of oxygen or to the valence change of Cu ions. The T_C onset values decrease also through the partial substitution of Zn for Cu. Akoshima et al. have shown that a combination of yttrium–zinc doping elements leads to drastic decrease of T_C [15] but this is beyond the scope of this paper. They attribute this phenomenon to a static stripe order. Indeed, this Zn cation can be seen as an impurity which is used like pinning centres of the possible dynamical stripe order leading to static stripe and a suppression of the superconductivity [14,15]. An important point is that a local minimum of T_C is observed for x' close to 0.33. As a matter of fact, this minimum corresponds to $p = \frac{1}{8}$ [15]. This result is also observed by XRD analysis. Indeed, for $x' = 0.33$, the FWHM of (001) peaks values are large, revealing more defect than for the other compositions. In fact, this x' value seems to be a kind of limit for Y atoms in a Bi2212 matrix. Beyond this limit, some clusters are formed in order to relax the internal strains.

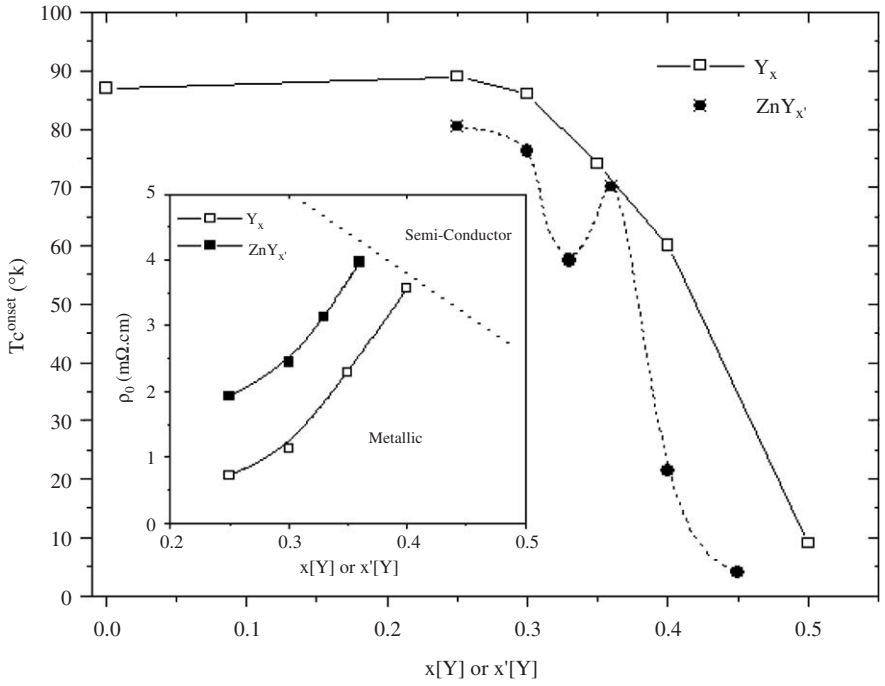

Fig. 10. Superconducting transition temperature (T_C onset) versus x (or x') for the Y_x (or $ZnY_{x'}$) compounds. Inset, residual resistivity ρ_0 versus x for both series.

4. Conclusion

Structural, microstructural and physical properties have been studied for different substituted Bi2212 powders in the family $Bi_2Sr_2Ca_{1-x}Y_xCu_2O_{8+\delta}$ (Y_x) and $Bi_2Sr_2Ca_{1-x'}Y_{x'}Cu_{1.94}Zn_{0.06}O_{8+\delta}$ ($ZnY_{x'}$). The structure of each compound can be described in the Bi2212 modulated framework. The diffraction peak broadening confirms that the crystalline structure is sensitive to the strains induced by the increase of Y substituting rate. Beyond a certain limit (x and $x' \approx 0.3$, 0.4), the FWHM decreases again, displaying a come back towards a structure showing fewer strains and then more relaxed. It can be noted that the critical temperature exhibits a minimum at x and x' close to 0.3, 0.4 prior collapsing. In the same way, the transport measurements show a crossover for x and x' close to 0.3, 0.4. This crossover separates a metallic conducting regime by scattering from a conducting regime by hopping between localized states (VRH). The stripe trapping, reported by Akoshima et al., might be related to an optimal distribution of the strains in the structure.

Acknowledgment

The authors express their gratitude to Dr. Sébastien Lambert for his help and fruitful discussion which helped to improve this paper.

References

[1] J.G. Bednorz, K.A. Muller, Z. Phys. B 64 (1986) 189.
[2] T. Janssen, A. Janner, A. Looijenga, P.M. de Wolff, in: A.J. Wilson (Ed.), International Tables for Crystallography C797, Kluwer Academic, Dordrecht, 1992.
[3] N. Jakubowicz, D. Grebille, M. Hervieu, H. Leligny, Phys. Rev. B 63 (2001) 214511.
[4] D. Grebille, H. Leligny, O. Pérez, Phys. Rev. B 64 (2001) 106501.
[5] A. Bianconi, M. Lusignoli, N.L. Saini, P. Bordet, Å. Kvick, P.G. Radaelli, Phys. Rev. B 54 (1996) 4310.
[6] A. Yamamoto, M. Onoda, E. Takayama-Muromachi, F. Izumi, T. Ishigaki, H. Asano, Phys. Rev. B 42 (1990) 4228.
[7] V. Petricek, Y. Gao, P. Lee, P. Coppens, Phys. Rev. B 42 (1990) 387.
[8] J. Etrillard, P. Bourges, C.T. Lin, Phys. Rev. B 62 (2000) 150.
[9] J.M. Perez-Mato, J. Etrillard, J.M. Kiat, B. Liang, C.T. Lin, Phys. Rev. B 67 (2003) 024504.
[10] J. Shimoyama, J. Kasa, T. Morimoto, J. Mizusaki, H. Tagawa, Physica C 185–189 (1991) 931.
[11] G. Marbach, S. Stotza, M. Klee, J.U.C. De Veries, Physica C 161 (1989) 111.
[12] K. Yamada, C.H. Lee, K. Kurahashi, J. Wada, S. Wakimoto, S. Ueki, H. Kimura, Y. Endoh, S. Hosoya, G. Shirane, R.J. Birgeneau, M. Greven, M.A. Kastner, Y.J. Kim, Phys. Rev. B 57 (1998) 6165.
[13] M.H.A. Mook, F. Dogan, B.C. Chakoumakos, Cond-mat/9811100.
[14] J.M. Tranquada, B.J. Sternlieb, J.D. Axe, Y. Nakamura, S. Uchiba, Nature (London) 375 (1995) 561.
[15] M. Akoshima, T. Noji, Y. Ono, Y. Koike, Phys. Rev. B 57 (1998) 7491.
[16] A. Douy, P. Odier, Mater. Res. Bull. 24 (1989) 1119.
[17] B. Pignon, E. Veron, J. Noudem, A. Ruyter, L. Ammor, I. Monot-Laffez, Physica C 434 (2006) 45.
[18] V. Petricek, M. Dusek, JANA 00: Programs for Modulated and Composite Crystals, Institute of Physics, Praha, Czeck Republic.
[19] J.M. Tarascon, W.R. McKinnon, P. Barboux, D.M. Hwang, B.G. Bagley, L.H. Greene, G.W. Hull, Y. LePage, N. Stoffel, M. Giroud, Phys. Rev. B 38 (1998) 8885.
[20] -2N. Fukushima, H. Niu, K. Ando, Jpn. J. Appl. Phys. 27 (1988) L1432.
[21] C.N.R. Rao, R. Nagarajan, R. Vijayaraghavan, N.Y. Vasanthacharva, G.V. Kulkarni, G. Rango Rao, A.M. Umarji, P. Somasundaram,

G.N. Subbanna, A.R. Raju, A.K. Sood, N. Chandrabhas, Supercond. Sci. Technol. 3 (1990) 242.
[22] Y. Inoue, Y. Shichi, F. Munakata, M. Yamanaka, Y. Koyama, Phys. Rev. B 40 (1989) 7307.
[23] C. Kendziora, L. Forro, D. Mandrus, J. Hartge, P. Stephens, L. Mihaly, R. Reeder, D. Moecher, M. Rivers, S. Sutton, Phys. Rev. B 45 (1992) 13025.
[24] A. Maeda, M. Hase, I. Tsukada, K. Noda, S. Takebayashi, K. Uchinokura, Phys. Rev. B 41 (1990) 6418.
[25] U. Staub, L. Soderholm, S. Skanthakumar, P. Pattison, K. Conder, Phys. Rev. B 57 (1998) 5535.
[26] A. Yamamoto, M. Onoda, E. Takayama-Muromachi, F. Izumi, T. Ishigaki, H. Asano, Phys. Rev. B 42 (1990) 4228.
[27] G.K. Williamson, W.H. Hall, Acta Metall. 1 (1953) 22.
[28] C. Quitmann, D. Andrich, C. Jarchow, M. Fleuster, B. Beschoten, G. Güntherodt, V.V. Moshchalkov, G. Mante, R. Manzke, Phys. Rev. B 46 (1992) 11813.